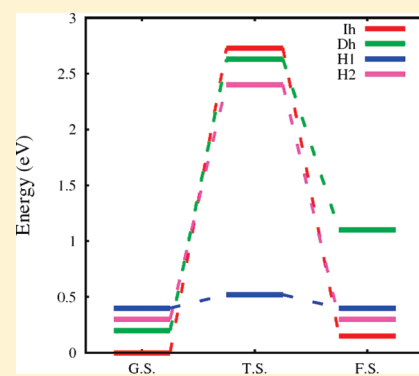


# Size- and Shape-Sensitive Reactivity Behavior of Al<sub>n</sub> (n = 2–5, 13, 30, and 100) Clusters Toward the N<sub>2</sub> Molecule: A First-Principles Investigation

Bhakti S. Kulkarni,<sup>†</sup> Sailaja Krishnamurthy,<sup>‡</sup> and Sourav Pal<sup>\*,†</sup><sup>†</sup>Physical Chemistry Division, National Chemical Laboratory, CSIR, Pune 411008<sup>‡</sup>Functional Materials Division, Electrochemical Research Institute, CSIR, Karaikudi 630 006

**ABSTRACT:** Reactivity of aluminum clusters has been found to exhibit size-sensitive variations. N<sub>2</sub> reduction is a hard process, and its dissociation on the Al surface is one of the few chemical methods available under nonhazardous conditions. In this context, we attempt to understand the adsorption behavior of N<sub>2</sub> molecules as a function of varying size and shape of Al clusters using a Density Functional Theory (DFT) based method. During the complex formation, various N<sub>2</sub> adsorption modes are examined. The results clearly demonstrate that, while the interaction energy does not vary with respect to the cluster size, shape of the cluster is highly contributive toward the chemisorption (a prerequisite for the reactivity) of the N<sub>2</sub> molecule. The underlying electronic and structural factors influencing the adsorption of N<sub>2</sub> molecules on the Al clusters are analyzed with the help of the Electron Localization Function (ELF) and Frontier Molecular Orbitals. As an illustration, the activation barrier calculations on various Al<sub>13</sub> conformations are calculated, and results confirm the experimental propositions that high-energy structures (depending upon their geometrical and electronic orientation) are more favorable for N<sub>2</sub> reduction.



## I. INTRODUCTION

During the last two decades, metallic nanoclusters have received considerable attention due to their finite size- and shape-dependent properties such as electronic structure,<sup>1,2</sup> thermodynamic stability,<sup>1,2</sup> magnetic behavior,<sup>1,2</sup> optical properties,<sup>3–5</sup> etc. Among the metallic clusters, aluminum nanoclusters,<sup>6,7</sup> aluminum nitrides,<sup>8</sup> and aluminum-based superatoms<sup>9,10</sup> have been important due to their renewed technological applications,<sup>11,12</sup> especially in the area of nanocatalysis.<sup>13</sup> For example, Al<sub>n</sub> (n = 16–18) clusters have shown dissociative chemisorption of water resulting in production of hydrogen gas.<sup>14</sup> Also, the dissociative chemisorption of molecular hydrogen on charged and neutral aluminum clusters has been modeled by Henry et al. They determined the comparative reaction barriers and enthalpies for both neutral and singly charged clusters.<sup>15,16</sup> Johnson et al.,<sup>17</sup> through combined experimental and theoretical exercises, have clearly demonstrated the importance of clusters as model systems for investigating nanoscale catalysis. These findings distinctly bring out the importance of structure on the adsorption and hence reactivity. Variance in the reactivity at nanoscale is due to an irregular charge distribution on the cluster surface which is further dependent on size and geometry (shape) of the cluster. Hence, the geometric and as a consequence the electronic stability of the cluster has been of great practical importance. Experimental and theoretical studies have shown that among the small aluminum clusters Al<sub>7</sub><sup>+</sup> and Al<sub>13</sub><sup>–</sup> are particularly stable<sup>18–21</sup> as their valence electron configurations approach closed-shell magic configurations.<sup>22,23</sup> Further, it has been proposed that adsorption of small molecules on unstable

clusters can provide the necessary extra electron to complete its electronic configuration and therefore may be suitable for the preparation of new cluster-assembled materials.<sup>24–29</sup>

In this context, several theoretical and experimental investigations have been carried out to understand the adsorption of small molecules such as H<sub>2</sub>O,<sup>14</sup> O<sub>2</sub>,<sup>30</sup> H<sub>2</sub>,<sup>20,31–35</sup> D<sub>2</sub>,<sup>36,37</sup> etc. on Al clusters. Reactivity trends are also quite important in the adsorption of N<sub>2</sub> molecules on Al clusters. This is because the activation of N<sub>2</sub> (nitrogen fixation) is a challenge due to its ample bond energy. In addition, aluminum nitride, one of the industrially important materials, carries a high impact as an electronic material and is usually synthesized through a direct reaction between the Al surface and N<sub>2</sub> at a high temperature and pressure.<sup>38,39</sup> Several previous studies report the general properties of small clusters formed by a mixture of Al and N atoms. For very small clusters like Al<sub>2</sub>N<sub>2</sub>, partial reduction of the N–N bond is observed which is associated with the formation of an anion N<sub>2</sub><sup>2–</sup> moiety rather than separated nitrido (N<sup>3–</sup>) anions.<sup>40–42</sup> In a computational study on M<sub>3</sub>N<sub>3</sub> clusters (M = Al, Ga, In), Kandalam et al.<sup>43</sup> found that ionic MN bonds are formed only in the case of M = Al. Aluminum is therefore a much better reducing agent for nitrogen than Ga and In, and the strength of the metal–nitrogen bond decreases in going from Al to In. Combined photoelectron spectroscopy and ab initio calculations by Averkiev et al.<sup>44,45</sup> show the formation of a N-centered

Received: April 13, 2011

Revised: June 11, 2011

Published: June 22, 2011

octahedral  $\text{Al}_6\text{N}^-$  and  $\text{Al}_7\text{N}^-$  cluster anions. Thus, in the small Al cluster sizes, the nitrogen impurity is absorbed (rather than adsorbed) by the metallic host. On the other hand, reports by Bai et al.<sup>46</sup> show that for larger clusters the nitrogen impurity prefers a peripheral position with just four Al–N bonds, which is the same as the coordination number for the Al atom in bulk aluminum nitride.

The importance of the Al–N reaction has motivated Romanowski et al.<sup>47</sup> to perform a theoretical study of  $\text{N}_2$  reaction with liquid Al metal. They have calculated the activation barrier for dissociative chemisorption of  $\text{N}_2$  to be 3.0 eV. At low temperatures, the  $\text{N}_2$  molecule is only known to physisorb on the Al surfaces. In another work, experimental studies<sup>48,49</sup> have shown that the high-energy configurations (obtained from the high-temperature conditions) have enhanced catalytic reactivity toward  $\text{N}_2$  molecules as compared to their ground state analogues when subjected to the same (room temperature) reaction conditions. In the case of the former, the activation barrier is seen to drop by nearly 1 eV. Despite the fact that the surface atoms in the liquid Al or high-energy Al conformations are at a lower energy and hence adjust easily to the incoming  $\text{N}_2$  molecule, there must be a clear correlation between the structure and reactivity/adsorption trends. Hence, in the present paper, we explore the reactivity of Al clusters using a nitrogen molecule. We address issues such as: Is the reactivity toward the  $\text{N}_2$  molecule a function of cluster size? Is the reactivity shape sensitive? Or, in other words, how does a structural change help in enhancing the reactivity of a given cluster size?

For this objective, we have chosen Al clusters with varying number of atoms and shapes. It includes lowest-energy conformers of  $\text{Al}_2$ ,  $\text{Al}_3$ ,  $\text{Al}_4$ ,  $\text{Al}_5$ ,  $\text{Al}_{13}$ ,  $\text{Al}_{30}$ , and  $\text{Al}_{100}$  clusters.  $\text{Al}_2$ – $\text{Al}_5$  are small Al clusters that have been analyzed for understanding the adsorption of the  $\text{N}_2$  molecule. The reason for starting with such small clusters is to have a qualitative understanding on two issues, viz., (a) the electronic properties underlying the adsorption of the  $\text{N}_2$  molecule on the cluster and (b) the adsorption of the  $\text{N}_2$  molecule as a function of size and orientation. The adsorption studies are extended to the high-energy conformations of  $\text{Al}_n$  ( $n = 3$ – $5$ , 13) clusters to evaluate shape sensitivity of  $\text{N}_2$  adsorption. All considered structures are optimized, and the bonding properties within them are analyzed through the Electron Localization Function (ELF) and Frontier Molecular Orbitals.

The rest of the work is organized as follows. In Section II, we give a brief description of the computational method and descriptors of reactivity used in this work. Results and discussion are presented in Section III for the  $\text{Al}_n$ – $\text{N}_2$  interaction. Finally, our conclusions are summarized in Section IV.

## II. COMPUTATIONAL DETAILS

As mentioned earlier, aluminum clusters of varying sizes, viz.,  $\text{Al}_2$ ,  $\text{Al}_3$ ,  $\text{Al}_4$ ,  $\text{Al}_5$ ,  $\text{Al}_{13}$ ,  $\text{Al}_{30}$ , and  $\text{Al}_{100}$ , are considered in the present study. Several initial conformations are generated for cluster sizes with atoms 3–5 and 13. For  $\text{Al}_{30}$  and  $\text{Al}_{100}$ , nearly 50 conformations are generated from various databases. All the generated conformations are optimized using a Density Functional Theory (DFT) based method. Following the optimization, low-lying structures and few characteristic high-energy conformations are considered for  $\text{N}_2$  adsorption. The optimization is carried out using VASP.<sup>50,51</sup> All the molecules are enclosed in a cubical box. The dimensions of the box are set to 10 Å greater than the largest diameter of the cluster. We have ensured that the

results are converged with respect to a further increase in the size of the simulation box. As in standard DFT programs, the stationary state (local minima) is calculated by iteratively solving Kohn–Sham equations.<sup>52</sup> Vanderbilt's ultrasoft pseudo-potentials<sup>53</sup> within the Local Density Approximation (LDA) are used for describing the behavior of core electrons. All LDA potentials apply the exchange correlation form according to Ceperly and Alder as parametrized by Perdew and Zunger, whereas the GGA potentials use the same parametrization and apply the generalized gradient corrections PW91.<sup>54a</sup> To validate the choice of functional,  $\text{Al}_2$  was initially optimized with both GGA and LDA functionals. The Al–Al bond distances obtained using both the methods are found to be 2.62 and 2.59 Å, respectively. Thus, LDA is seen to give closer  $\text{Al}_2$  interatomic distances with respect to the experimental value of 2.56 Å.<sup>1</sup> Hence, all further calculations were done using the LDA method. Further validation of the used method is done by comparing the ground state geometries, the Al–Al bond lengths, and relative energies such as cohesive and atomization energies with that of high-level benchmark results.<sup>54b</sup> An energy cutoff of 400 eV has been used for the plane-wave<sup>54</sup> expansion of Al and N atoms. The structural optimization of all geometries is carried out using the conjugate gradient method<sup>55</sup> except for the high-energy conformers where the *quasi-Newton* method<sup>56</sup> is used to retain the local minima. The structure is considered to be optimized when the maximum force on each atom is less than 0.001 eV/Å. The frequency analysis was performed on all stationary points, and no imaginary frequency was observed.

The Electron Localization Function (ELF)<sup>57</sup> is applied to describe the nature of bonding within the aluminum clusters as well as Al–N complexes. According to a description by Silvi and Savin,<sup>57</sup> the molecular space is partitioned into regions or basins of localized electron pairs or attractors. At a very low value of ELF, all the basins are connected. As this value increases, the basins begin to split, and finally, we will get as many basins as the number of atoms. Typically, the existence of an isosurface in the bonding region between two atoms at a high value of ELF, say around 0.70 and above, signifies a localized bond in that region. The mathematical description of ELF is as follows

$$\eta(r) = \frac{1}{1 + \left(\frac{D_p}{D_h}\right)^2} \quad (1)$$

$$D_h = \left(\frac{3}{10}\right) (3\pi^2)^{5/3} \times \rho^{5/3} \quad (2)$$

$$D_p = \frac{\frac{1}{2} \sum_i |\nabla\Psi|^2 - \frac{1}{8} |\nabla\rho|^2}{\rho} \quad (3)$$

$$\rho = \sum_{i=1}^N |\psi(r)|^2 \quad (4)$$

where  $D_p$  stands for the excess local kinetic energy due to the Pauli restriction, i.e., the difference between the definite positive kinetic energy density  $T_s(\mathbf{r})$  of the actual fermionic system and that of the von Weizsäcker kinetic energy functional  $T_W(\mathbf{r})$ . If the wave function is written as a single determinant,  $D_p$  is

expressed in terms of orbital contributions as in eq 3.  $D_h$  is the kinetic energy of the electron gas having the same density, or one can say it is the value of  $D_p$  in a homogeneous electron gas, and  $\rho$  is the charge density.

### III. RESULTS AND DISCUSSION

**(A). Adsorption Behavior of the  $N_2$  Molecule on Aluminum Clusters.** (i). *Structural, Electronic, and Adsorption Properties of  $Al_n$  ( $n = 2-5$ ) Clusters.* The  $Al_2$  dimer and small-sized Al atomic clusters,<sup>58-61</sup> viz.,  $Al_3$ ,  $Al_4$ , and  $Al_5$ , are widely studied to understand the adsorption of molecules such as  $H_2O$ ,<sup>14</sup>  $O_2$ ,<sup>30</sup>  $H_2$ ,<sup>20,31-35</sup>  $D_2$ ,<sup>36,37</sup> etc. In the present work, we first analyze the size dependence of the  $N_2$  interaction on these small-sized Al clusters. The  $N_2$  molecule can adsorb on the  $Al_n$  clusters through three different modes, viz., (a) along the Al–Al bond which we call “linear mode”, (b) parallel to the Al–Al bond which we call “parallel mode”, and (c) perpendicular to the Al–Al bond. The (a) and (b) modes of adsorption result in a stable complex with varying strength of interaction for all  $Al_n$  clusters; however, the perpendicular mode of adsorption results in a metastable complex for all the clusters.

The ground state geometry and ELF contours of  $Al_2$  along with a demonstration of different modes of  $N_2$  adsorption are given in Figure 1(a). As can be seen from Figure 1(a), the interatomic bond distance in  $Al_2$  is 2.59 Å. The covalent nature of this bond is clearly understood from its ELF contour. The two atomic basins merge at an isovalue of 0.78. Coming to the  $Al_2-N_2$  complexes, in “linear” mode,  $N_2$  is adsorbed on the  $Al_2$  with an Al–N bond distance of 1.86 Å. Following the adsorption, the N–N bond elongates from 1.11 to 1.15 Å. Similarly, the Al–Al bond shows a marginal increase of around 0.03 Å. The ELF isosurface at a value of 0.78 for the complex shows polarized basins on the interacting Al and N atoms (see Figure 1(a)). The basins along the Al–Al bond and N–N bond merge by an isovalue of 0.70, while the basins of the adjacent Al and N atoms do not merge even at an isovalue of 0.50. Therefore, the Al–N bond formed in this complex is far from covalent in nature. The polarization of basins, on the other hand, shows the Al–N bond to be weakly ionic in nature. This analysis is also supported by the interaction energy value, which is around 13 kcal/mol.

On the other hand, the “parallel mode” of adsorption results in a stable  $Al_2-N_2$  complex with interaction energy of 38.51 kcal/mol. The complex has three Al–N bonds which vary from 1.93 to 2.14 Å (see Figure 1(a)). Further, the Al–Al and N–N bond lengths elongate by 0.34 and 0.1 Å, respectively. These geometrical parameters correspond very well to the earlier reported values on  $(AlN)_2$  polyatomic clusters<sup>42</sup> where Al–N and N–N distances in  $D_{\infty h}$  symmetry correspond to 2.10 and 1.29 Å, respectively. In this case, the ELF basins along the Al–N bond merge at an isovalue 0.72, thereby demonstrating it to be covalent in nature. The Al–Al basins in the complex also merge at high isovalue of 0.82. Thus, the ELF contours and shorter bond lengths indicate toward an increased covalent nature and thereby stability of the “parallel mode” complex as compared to the “linear mode” complex.

The ground state geometries of  $Al_3$ ,  $Al_4$ , and  $Al_5$  are shown in Figure 1(b). Cyclic  $Al_3$  (ground state geometry of  $Al_3$ ) is an equilateral triangle with all Al–Al bond distances around 2.47 Å.  $Al_4$  and  $Al_5$  ground state geometries are built upon the  $Al_3$  ground state geometry with Al–Al bond distances along the vertices varying between 2.47 and 2.60 Å. The interatomic

distances between the diagonal atoms are 2.79 and 2.81 Å in  $Al_4$  and  $Al_5$  clusters, respectively. This bonding pattern reflects in ELF where the basins along the surface bonds merge by an isovalue of 0.82 for  $Al_3$  (all the bonds are surface bonds),  $Al_4$ , and  $Al_5$ . On the other hand, the basins along the diagonal bonds in  $Al_4$  and  $Al_5$  merge only around an isovalue of 0.72. Thus, the bonds along the surface are more covalent in nature, while the diagonal bonds are more metallic (and less covalent) in nature with their values being close to those found in bulk aluminum which is around 2.86 Å.<sup>62</sup>

Linear and parallel modes of  $N_2$  adsorption are studied on the ground state geometries of  $Al_3$ ,  $Al_4$ , and  $Al_5$  clusters. We first discuss the outcome of the linear mode of adsorption on these ground state geometries.  $N_2$  is adsorbed linear to one of the Al–Al bonds on various sites of these small-sized clusters. Figure 1(b) shows the most favorable sites of adsorption for  $N_2$  on  $Al_3$ ,  $Al_4$ , and  $Al_5$  ground state geometries. As in the case of  $Al_2$ , the linear mode of adsorption on all of the three ground state geometries results in a complex with reasonably low interaction energy of  $\sim 8$  kcal/mol. The geometrical modifications are similar as those noted in the case of the  $Al_2-N_2$  linear mode complex. Surprisingly, the parallel mode of adsorption on  $Al_3$ ,  $Al_4$ , and  $Al_5$  ground state geometries does not result in an appreciable interaction energy which ranges between 8 and 13 kcal/mol. For instance, interaction of the  $Al_4$  ground state geometry with  $N_2$  in parallel mode leads to two Al–N bonds with lengths of 2.23 and 2.38 Å, respectively. However, the N–N bond after the formation of complex elongates by just 0.04 Å. The reason for this low interaction even in the parallel mode may be attributed to a slightly higher degree of covalency in these clusters (as indicative by slightly smaller Al–Al bond distances and the value at which ELF basins merge along the surface atoms) that does not favor an  $N_2$  adsorption.

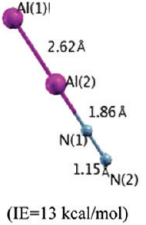
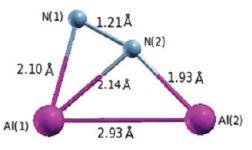
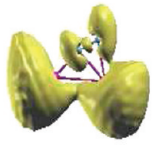
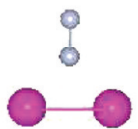
In addition to the ground state  $Al_n$  clusters,  $N_2$  adsorption is also studied on several high-energy  $Al_n$  ( $n = 3-5$ ) conformations. The high-energy structures chosen differ nearly by 1.13 to 1.83 eV in energy compared to their ground state analogues. Figure 1(c) shows few characteristic high-energy conformations studied, the bonding within them through ELF contours, and  $Al_n-N_2$  complexes with their interaction energies. The high-energy conformations of  $Al_n$  ( $n = 3-5$ ) clusters show a lower symmetry as compared to their ground state counterparts. As an illustration, we discuss the high-energy conformations of  $Al_3$ , viz., the bent and linear conformations. In linear structure, the two Al–Al bonds are nearly equivalent, and ELF basins of all three atoms merge at an isovalue of 0.84. On the contrary, the two bond distances in the bent structure vary by 0.12 Å. In line with that, Al(1)–Al(3) basins merge at an isovalue of 0.86, while the Al(1)–Al(2) basins merge at an isovalue of 0.78 (figure not shown). Similarly, the atoms in various high-energy conformations of  $Al_4$  and  $Al_5$  are bonded to each other through a larger range of bond lengths (see Figure 1(c)). Some of the ELF basins in these high-energy conformations begin to merge at much higher isovalue (around 0.86) as compared to those in the ground state conformation, while some other basins merge at considerably lower isovalue (around 0.72 and below). Thus, the high-energy conformations have enlarged covalent bonding at specific pockets with the remaining parts exhibiting a more metallic (or lower covalent) bonding.

The linear mode of adsorption on several high-energy conformations is seen to give results very similar to that of their ground state counterparts with interaction energies varying

between 6 and 11 kcal/mol. However, the corresponding parallel mode of adsorption results in very stable  $Al_n-N_2$  ( $n = 3-5$ ) complexes with interaction energies of 30 kcal/mol and above.

Incidentally, all the favorable parallel adsorption modes are along the more weakly bonded Al–Al bonds of the Al cluster. For instance, a favorable parallel adsorption of  $N_2$  on  $Al_4$  is seen only

a)

Modes of Adsorption	$Al_n$	ELF
-		 (isovalue=0.78)
Linear		 (isovalue=0.78)
Parallel		 (isovalue=0.72)
Perpendicular		Failed to form complex

b)

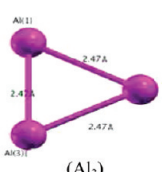
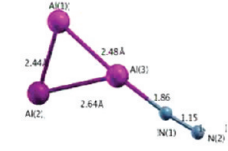
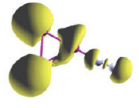
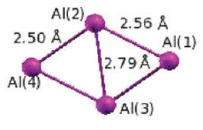
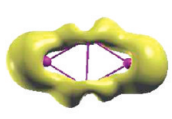
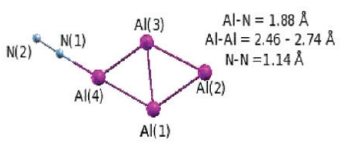
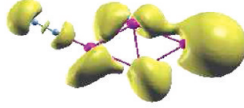
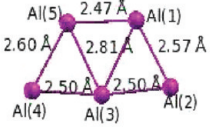
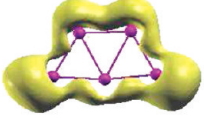
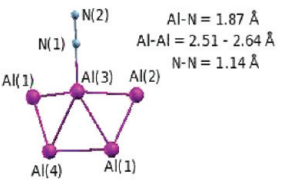
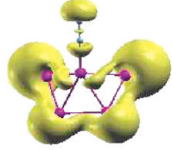
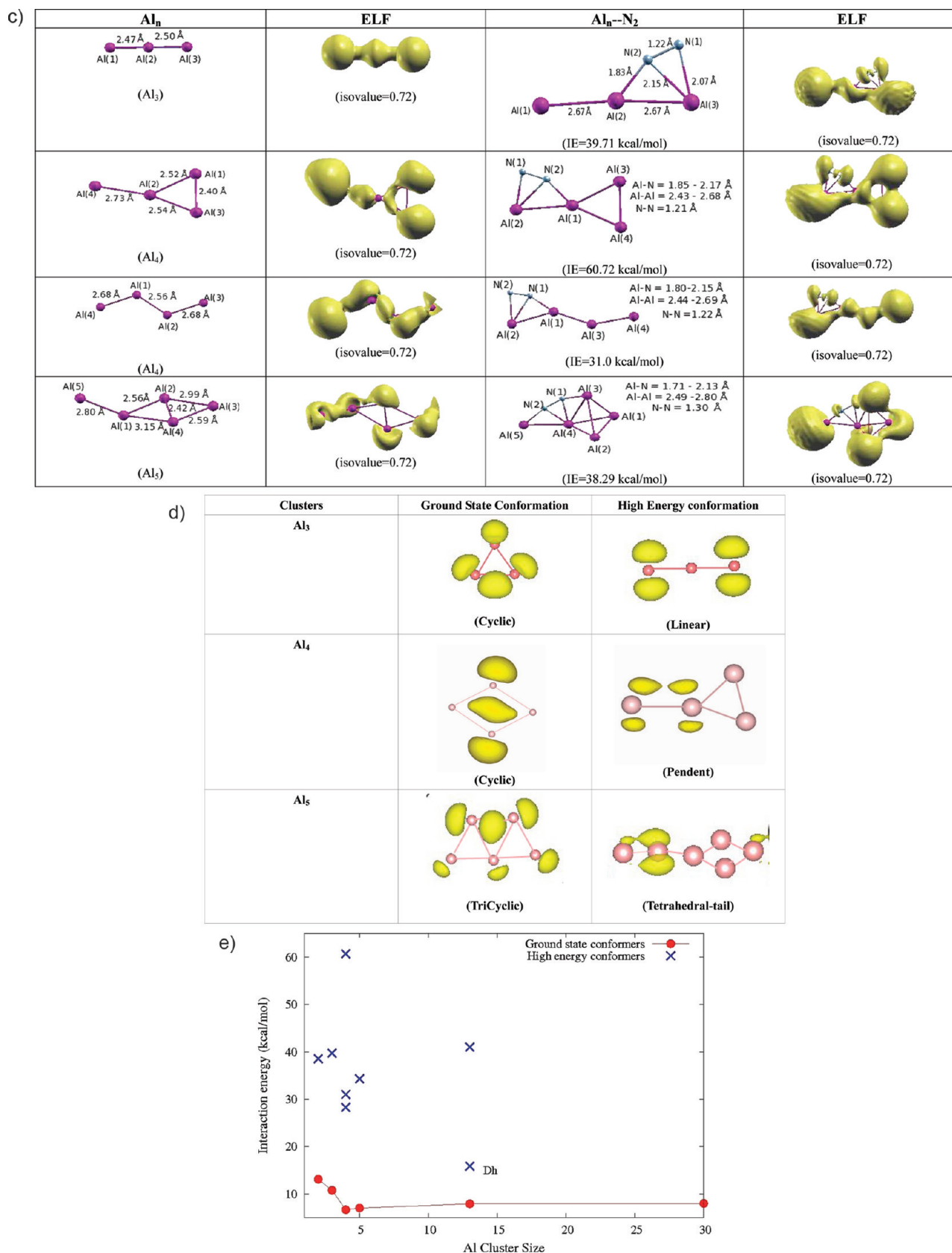
$Al_n$	ELF	$Al_n-N_2$	ELF
 ( $Al_3$ )	 (isovalue=0.82)		 (isovalue=0.82)
 ( $Al_4$ )	 (isovalue=0.82)		 (isovalue=0.82)
 ( $Al_5$ )	 (isovalue=0.82)		 (isovalue=0.82)

Figure 1. Continued



**Figure 1.** (a) Ground state geometries, ELF of the  $Al_2$  cluster, and its corresponding  $N_2$  complex. (b) Ground state geometries, ELF of  $Al_n$  ( $n = 3-5$ ) clusters, and their corresponding  $N_2$  complexes. (c) High-energy conformer geometries and ELF of  $Al_n$  ( $n = 3-5$ ) clusters and their corresponding  $N_2$  complexes. (d) LUMO contribution for  $Al_n$  clusters in ground state and high-energy conformations. (e) Interaction energy with the  $N_2$  molecule as a function of Al cluster size and conformation.

along the Al(4) and Al(2) bond (see Figure 1(c)). Parallel adsorption of N<sub>2</sub> along Al(2)–Al(1), Al(1)–Al(3), and Al(2)–Al(3) bonds results in complexes with lower interaction energies. Thus, the parallel adsorption of N<sub>2</sub> on high-energy Al conformations is site and geometry specific. The high-energy conformations with short Al–Al bonds along the surface do not favor N<sub>2</sub> adsorption (interaction energies in these cases vary between 5 and 10 kcal/mol), whatever the adsorption mode. In the case of complexes with high interaction energies of 30 kcal/mol and above, the numbers of Al–N bonds formed are as good as that noted in bulk aluminum nitride. In these cases, the ELF basins along the Al–N bond merge at an isovalue of 0.72, predicting the Al–N bond to be predominantly covalent. Further, the interacting Al–Al bonds and N–N bonds elongate by about  $\sim 0.25$  and  $\sim 0.1$  Å in comparison to those in the bare cluster. In addition to the structural analysis, the interaction energy of  $\sim 40$  kcal/mol for these complexes strengthens the feasibility of a polyatomic cluster formation. To support our above structural analysis, we also examine the Frontier Molecular Orbital (FMO) contribution which is known to be a good reactivity descriptor. Figure 1(d) illustrates the LUMO contribution for Al<sub>n</sub> clusters in their respective ground state conformations and high-energy conformations. As an example, we elaborate LUMO discussion of ground state cyclic and high-energy pendent conformation of the Al<sub>4</sub> cluster. It is clearly seen from Figure 1(d) that in the case of high-energy conformers the p-orbitals of the adjacent Al atoms contribute to the LUMO of the cluster. This results in a strong  $\pi$ – $\pi$  type overlap between the LUMO of the cluster and the HOMO of the N<sub>2</sub> molecule. The same site specifications are observed for the Al<sub>2</sub> cluster, where its LUMO is p-orbital concentrated on two Al atoms, which eventually leads to higher interaction with incoming N<sub>2</sub> molecule in parallel mode. Nonetheless, the ground state geometries of other clusters fail to achieve this specific site requirement due to their symmetric nature and hence better hybridization between the s and p atomic orbitals within them (as shown for cyclic conformation of Al<sub>4</sub> in Figure 1(d)).

We conclude the results of this section in Figure 1(e), which gives the interaction energy between the N<sub>2</sub> molecule and Al clusters as a function of cluster size and shape. Thus, the reactivity of Al clusters toward the N<sub>2</sub> molecule is not size sensitive; rather, it is shape and site sensitive. As the number of atoms increases, the high-energy conformers provide distinct shapes with varying bonding pattern within it thereby leading to distinct reactive sites. In other words, the variation of the bonding within the Al atoms in the high-energy conformations facilitates easier adsorption of the N<sub>2</sub> molecule at specific sites, where the Al–Al bonds are more weakly bonded at a few pockets in the cluster (i.e., bonded through larger interatomic distances in the range of 2.79–3.10 Å). Also, the parallel mode of adsorption facilitates the formation of multiple Al–N bonds at sites with larger Al–Al distances of a given cluster.

(ii) *Structural, Electronic, and Adsorption Properties of Al<sub>n</sub> (n = 13, 30, 100) Clusters.* Next we consider somewhat larger aluminum clusters for N<sub>2</sub> adsorption. Al<sub>13</sub> is the most well studied among the aluminum clusters. Icosahedra (Ih) is found to be the global minima of Al<sub>13</sub> in this study as well as in all earlier studies.<sup>50</sup> Hence, we found it interesting to choose this cluster for N<sub>2</sub> adsorption. In addition, there are several reports for the clusters with 30–100 atoms.<sup>6,48,63,64</sup> There have been quite a few contrasting reports on the lowest-energy conformation of Al<sub>30</sub>. One of the reports suggests a double tetrahedron as a global

minima for Al<sub>30</sub>.<sup>63</sup> Recent reports, on the other hand, predict a structure built upon a hexagonal motif as the lowest-energy geometry for Al<sub>30</sub>.<sup>64,6</sup> The ground state geometry obtained in our case is seen to agree with the reports of Drebov et al.<sup>64</sup> with double tetrahedron nearly 8.5 kcal/mol higher in energy as compared to the structure based on the hexagonal motif. Hence, we discuss here the structural and bonding features in the hexagonal motif conformation followed by the N<sub>2</sub> adsorption on it. While it is difficult to guarantee global minima for a 100 atom cluster, we propose the conformation discussed in this work as a potential minima of Al<sub>100</sub>. It is difficult to illustrate in detail structural parameters of a 100 atom cluster and their corresponding N<sub>2</sub> complexes; hence, we only outline the bonding as predicted by ELF. Figure 2(a) shows the optimized ground state geometries and ELF contours of 13, 30, and 100 atom clusters and their N<sub>2</sub> complexes.

The ground state geometry of Al<sub>13</sub> has three unique reactive sites, namely, “A”, “B”, and “C”, as shown in Figure 2(a). These reactive sites arise due to their distinct distances from the central atom. The atoms “B” and “C” are at 2.66 and 2.60 Å from the central atom “A”, respectively. Hence, it is clearly seen that the global minimum of the Al<sub>13</sub> cluster is not a perfect Ih but includes slight Jahn–Teller distortion leading to the D<sub>3d</sub> structure. A distance between two adjacent “B” atoms is 2.82 Å, while that of two adjacent “C” atoms is 2.90 Å. The interatomic distance between sites “B” and “C” is 2.70 Å. On the contrary, in Al<sub>30</sub> ground state geometry, surface atoms result in shorter bond length ranging from 2.53 to 2.74 Å, whereas core atoms are interconnected through longer bond lengths of 2.71–2.87 Å. In the Al<sub>100</sub> cluster, the Al–Al bond lengths vary between 2.63 and 3.15 Å with surface atoms interconnected through shorter bond distances.

Analysis of ELF for Al<sub>13</sub> shows that the ELF basins do not merge up to an isovalue of 0.75. Around 0.74, basins of “B” and “C” atoms merge with each other, while the basins along “B–B” and “C–C” bonds merge at a slightly lower isovalue of 0.72. In the case of Al<sub>30</sub>, at an isovalue of 0.86, the basins of all surface atoms merge, while the basins of core atoms merge at a lower value of 0.74. The covalency of the Al<sub>100</sub> cluster is as good as that of the Al<sub>30</sub> cluster. The basins on the surface atoms of Al<sub>100</sub> start merging at an isovalue of 0.84. These results indicate an overall covalent nature of bonding, especially between the surface atoms in the moderate-sized Al<sub>n</sub> clusters (similar to that of small-sized clusters).

As in the case of smaller clusters, we consider two modes of N<sub>2</sub> interaction. The first case, where N<sub>2</sub> is kept linear to one of the Al–Al bonds in Al<sub>13</sub>, Al<sub>30</sub>, and Al<sub>100</sub>, results in a stable complex. Here, the Al–N bond distance is optimized to 1.90 Å as compared to 1.86 Å in Al<sub>n</sub> (n = 2–5)–N<sub>2</sub> complexes. The N–N bond elongation in the complex is 1.13 Å as compared to 1.15 Å in Al<sub>2</sub> and Al<sub>3</sub>. The interacting Al–Al bond elongates by about  $\sim 0.03$  Å. Following the N<sub>2</sub> adsorption, there is a small loss of symmetry in each of these clusters. For example, the Al–Al bonds in the upper half of Ih-Al<sub>13</sub> elongate by about 0.03 Å. Consequently, the overall volume of the cluster increases to some extent. As anticipated once again, in this linear mode of N<sub>2</sub> adsorption there are no merged basins along the Al–N bond. However, the basins of Al atoms in the complex begin to merge around 0.76 in Al<sub>13</sub> and around 0.86 in Al<sub>30</sub> and Al<sub>100</sub>. Thus, the Al<sub>n</sub>–N<sub>2</sub> complex is a weak ionic one with interaction energy of  $\sim 7.50$  kcal/mol. Remarkably, this is nearly half of that found for the O<sub>2</sub> molecule on Al<sub>13</sub> (0.77 eV).<sup>30</sup> The parallel mode of N<sub>2</sub>

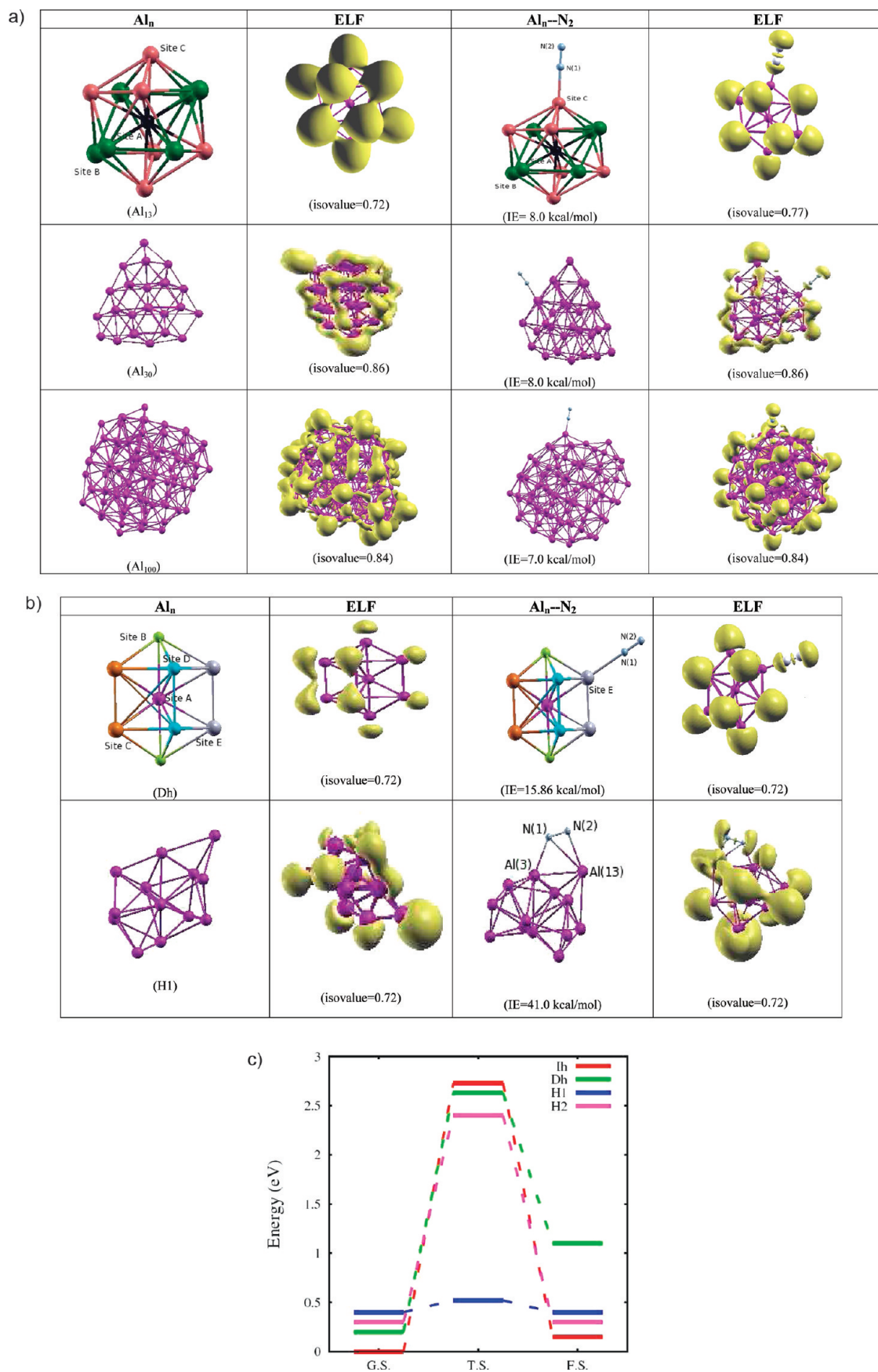


**Figure 2.** (a) Ground state geometries, ELF of  $Al_n$  ( $n = 13, 30, 100$ ) clusters, and their corresponding  $N_2$  complexes. (b) High-energy conformer geometries, ELF of  $Al_n$  ( $n = 13$ ) clusters, and their corresponding  $N_2$  complexes. (c) Activation barrier of  $N_2$  on various  $Al_{13}$  conformations.

adsorption on these clusters is found to be unstable with N<sub>2</sub> adsorbing only on one Al atom (resulting back into a linear mode of adsorption) with more or less the same interaction energy. Thus, the reactivity of ground state Al clusters is not size sensitive.

In view of the conclusion in the earlier section that the adsorption is sensitive to shape of the aluminum cluster, we study N<sub>2</sub> adsorption on a few characteristic high-energy Al<sub>13</sub> conformations. The next considered high-energy structures are roughly 0.34–2.56 eV higher in energy compared to the global minimum structure. Decahedron (Dh) is a dominant high-energy conformation of Al<sub>13</sub> seen between 400 and 1200 K in a finite temperature study.<sup>65</sup> Hence, we found it interesting to study the adsorption of N<sub>2</sub> on this conformation. In addition, we have also chosen quite a few high-energy conformations from a finite temperature run of Ih geometry at 1600 K and studied the N<sub>2</sub> adsorption on them. We discuss the results of one such characteristic high-energy conformation, viz., H1. Figure 2(b) shows the geometry and ELF of these high-energy conformations and their corresponding N<sub>2</sub> complexes. We have attempted both the linear and parallel modes of N<sub>2</sub> adsorption on these high-energy conformations. However, as the linear mode of adsorption leads to results very similar to those of small-sized high-energy Al conformations (i.e., high-energy conformations of Al<sub>3</sub>, Al<sub>4</sub>, and Al<sub>5</sub>), the details of those complexes are omitted in the further discussion.

When N<sub>2</sub> is adsorbed in parallel mode on the Dh conformation, it fails to form more than one Al–N bond on adjacent reactive sites. The resulted Dh–N<sub>2</sub> complex shows structural and ELF characteristics similar to that of the original Ih–N<sub>2</sub> complex. The interaction energy comes out to be 15.86 kcal/mol. On the other hand, the high-energy conformer, H1, forms a stable complex with the parallelly placed N<sub>2</sub>. The complex is characterized by the presence of two Al–N bonds (2.03 and 2.16 Å, respectively). The N–N bond elongates to 1.20 Å. The resulting interaction energy is 41 kcal/mol. The ELF basins along the Al–N and Al–Al bonds merge at an isovalue of 0.72 and 0.82, respectively. Therefore, for H1 (and a few other high-energy conformers), the enhanced interaction energy and covalency along the Al–N bond helps in chemisorption of N<sub>2</sub> (see Figure 1(e)). In other words, the high-energy conformers provide deformed structures where some of the adjacent Al–Al bonds are not so strongly coordinated. Around these sites, N<sub>2</sub> gets easily embedded in the cluster, forming various Al–N bonds and resulting in a stable (Al)<sub>n</sub>–N<sub>2</sub> complex. This is validated by the analysis of average interatomic Al–Al distances in Al clusters. For example, the average interatomic distance in the high-energy conformation of Al<sub>13</sub>, viz., H1, is 3.91 Å as compared to 3.59 and 3.65 Å in Ih and Dh, respectively.

**(B). Activation Barriers for the N<sub>2</sub> Molecule on Al<sub>13</sub> Conformations.** Relevance of calculations presented in the previous section can be verified by evaluating the activation barrier for N<sub>2</sub> adsorption. Hence, we have calculated the activation barriers on various Al<sub>13</sub> conformations and demonstrate the same on the ground state conformation of Al<sub>13</sub> and three high-energy conformations, viz., Dh, H1, and H2 (another high-energy Al<sub>13</sub> conformation) in Figure 2(c). The activation barriers are calculated using the Nudged Elastic Band (NEB) method as incorporated in VASP. The activation barrier for Ih is 2.73 eV, while that for Dh is 2.65 eV. However, the activation barrier for H1 is lower and is around 0.12 eV. Here, the activation barrier drops by 2.61 eV, i.e., 60.03 kcal/mol compared to that of Ih. The barrier is also

calculated on various other high-energy conformations of Al<sub>13</sub>. This value is found to be highly sensitive to the particular structural arrangement with some of the conformations showing a sizable drop in activation barrier. For example, on another high-energy conformer H2, the activation barrier results in 2.40 eV, thus it drops by 0.33 eV. The conformations with a lower activation barrier are characterized by the presence of weakly bonded Al–Al atoms along the surface of the cluster. Interestingly, this is in line with some of the recent experimental findings, which report the activation barrier to drop by nearly 1 eV on Al clusters subject to phase transition.<sup>48,49</sup> In the present study, the difference in the activation energy for the N<sub>2</sub> molecule on high-energy and ground state conformers of Al<sub>13</sub> and the fact that the N–N bond elongates systematically to 1.20 Å in several high-energy Al cluster–N<sub>2</sub> complexes following the adsorption present a consistent picture. Finally, we note that the activation barrier for N<sub>2</sub> on high-energy Al clusters is not very far away as compared to the values seen on various metal surfaces (between 0.2 and 0.8 eV<sup>66–69</sup>). It can thus be proposed that high-energy Al conformations with mixed bonding nature are better candidates for the Al–N polyatomic cluster formation and N<sub>2</sub> dissociation. Finally, it is interesting to state that our ELF results match with the Reigonal-DFT results studied by Yarovsky and co-workers.<sup>70</sup> This method provides a measure of the electronic stress tensor from which it is possible to determine bond indices and electronic chemical potential of Al clusters. Their calculated bond indices on the surface of Al<sub>12</sub>X clusters present a similar understanding of the mixed, covalent, and metallic bonding nature of the cluster. Similar to our ELF observations, these indices predict the regioselectivity observed in reactions of the Al clusters.

#### IV. CONCLUSION AND SCOPE

DFT-based calculations have been carried out to understand the reactivity of the Al<sub>n</sub> clusters ( $n = 2–5, 13, 30, 100$ ) toward the nitrogen molecule. The ground state and few high-energy conformers of Al<sub>n</sub> clusters are considered for this purpose. In addition, different modes of N<sub>2</sub> adsorption have been verified. For all ground state Al<sub>n</sub> conformers (except Al<sub>2</sub>), interaction energy is nearly constant irrespective of the N<sub>2</sub> adsorption mode. However, for high-energy Al<sub>n</sub> conformers, interaction is sensitive to the shape and the orientation of the N<sub>2</sub> molecule. High-energy conformers with nonuniform Al–Al bonds on the surface (more weakly bonded Al–Al bonds) provide strong sites for embedding of the N<sub>2</sub> molecule. This adsorption is accompanied by the formation of multiple covalent Al–N bonds and hence a highly stable (Al)<sub>n</sub>–N<sub>2</sub> complex. This is validated by the ELF contours where basins along the Al–N bond merge by an isovalue of 0.72. Interestingly, the activation barrier drops to 0.12–2.65 eV for high-energy and ground state conformers, respectively, thereby indicating the high-energy conformations to be better candidates for N<sub>2</sub> activation or formation of polyatomic Al–N compounds.

#### ■ AUTHOR INFORMATION

##### Corresponding Author

\*E-mail: s.pal@ncl.res.in.

#### ■ ACKNOWLEDGMENT

One of the authors (BSK) acknowledges CSIR (Council of Scientific and Industrial Research) for funding of the SRF

(Senior Research Fellowship). We acknowledge the Center of Excellence in Scientific Computing at NCL and High Performance Computing at CECRI. SP acknowledges the J. C. Bose Fellowship grant of DST towards partial fulfillment of this work. We acknowledge Dr. N. Drebov (Institut für Physikalische Chemie, Karlsruher Institut für Technologie (KIT), Kaiserstrasse 12, 76131 Karlsruhe, Germany) for providing us with several Al<sub>30</sub> conformations.

## REFERENCES

- (1) Khanna, S. N.; Jena, P. *Phys. Rev. Lett.* **1992**, *69*, 1664.
- (2) Khanna, S. N.; Jena, P. *Phys. Rev. B* **1995**, *51*, 13705.
- (3) Landman, U.; Luedtke, W. D.; Burnham, N. A.; Colton, R. J. *Science* **1990**, *248*, 454.
- (4) Yang, Y.; Chen, S. *Nano Lett.* **2003**, *3*, 75.
- (5) Pyykko, P. *Inorg. Chim. Acta* **2005**, *358*, 4113.
- (6) Aguado, A.; Lopez, J. M. *J. Chem. Phys.* **2009**, *130*, 064704.
- (7) Khanna, S. N.; Jena, P. *Chem. Phys. Lett.* **1994**, *219*, 479.
- (8) Costales, A.; Blanco, M. A.; Francisco, E.; Pends, A. M.; Pandey, R. *J. Phys. Chem. B* **2006**, *110*, 40925.
- (9) Akutsu, M.; Koyasu, K.; Atobe, J.; Hosoya, N.; Miyajima, K.; Mitsui, M.; Nakajima, A. *J. Phys. Chem. A* **2006**, *110*, 12073.
- (10) Reber, A. C.; Khanna, S. N.; Castleman, A. W. *J. Am. Chem. Soc.* **2007**, *129*, 10189.
- (11) Pasupathy, A. N.; Bialczak, R. C.; Martinek, J.; Grose, J. E.; Donev, L. A. K.; McEuen, P. L.; Ralph, D. C. *Science* **2004**, *306*, 86.
- (12) Nakamura, S. *Proceedings of International Symposium on Blue Laser and Light Emitting Diodes*; Yoshikawa, A., Kishino, K., Kobayashi, M., Yasuda, T., Eds.; Chiba University Press: Japan, 1996; p 119.
- (13) Valden, M.; Lai, X.; Goodman, D. W. *Science* **1998**, *281*, 1647.
- (14) Roach, P. J.; Woodward, W. H.; Castleman, A. W., Jr.; Reber, A. C.; Khanna, S. N. *Science* **2009**, *323*, 492.
- (15) Henry, D. J.; Yarovsky, I. *J. Phys. Chem. A* **2009**, *113*, 2565.
- (16) Henry, D. J.; Varano, A.; Yarovsky, I. *J. Phys. Chem. A* **2009**, *113*, 5832.
- (17) Johnson, G. E.; Mitrio, R.; Bonacic-Koutecky, V.; Castleman, A. W., Jr. *Chem. Phys. Lett.* **2009**, *475*, 1.
- (18) Rao, B. K.; Jena, P. *J. Chem. Phys.* **1999**, *111*, 1890.
- (19) Ahlrichs, R.; Elliott, S. D. *Phys. Chem. Chem. Phys.* **1998**, *1*, 13.
- (20) Cox, D. M.; Trevor, D. J.; Whetten, R. L.; Kaldor, A. *J. Phys. Chem.* **1988**, *92*, 421.
- (21) Taylor, K. J.; Pettiette, C. L.; Craycraft, M. J.; Chesnovsky, O.; Smalley, R. E. *Chem. Phys. Lett.* **1988**, *152*, 347.
- (22) Knight, W. D.; Clemenger, K.; de Heer, W. A.; Saunders, W. A.; Chou, M. Y.; Cohen, M. L. *Phys. Rev. Lett.* **1984**, *52*, 2141.
- (23) Chou, M. Y.; Cohen, M. L. *Phys. Lett.* **1986**, *113A*, 420.
- (24) Burkart, S.; Blessing, N.; Klipp, B.; Möller, J.; Ganteför, G.; Seifert, G. *Chem. Phys. Lett.* **1999**, *301*, 546.
- (25) Kawamura, H.; Kumar, V.; Sun, Q.; Kawazoe, Y. *Phys. Rev. B* **2001**, *65*, 045406.
- (26) Mañanes, A.; Duque, F.; Méndez, F.; López, M. J.; Alonso, J. A. *J. Chem. Phys.* **2003**, *119*, 5128.
- (27) Yarovsky, I.; Goldberg, A. *Mol. Simul.* **2005**, *31*, 475.
- (28) Han, Y.-K.; Jung, J.; Kim, K. H. *J. Chem. Phys.* **2005**, *122*, 124319.
- (29) Jung, J.; Han, Y.-K. *J. Chem. Phys.* **2006**, *125*, 064306.
- (30) Reber, A. C.; Khanna, S. N.; Roach, P. J.; Woodward, W. H.; Castleman, A. W., Jr. *J. Am. Chem. Soc.* **2007**, *129*, 16098.
- (31) Li, Z. J.; Li, J. H. *Solid State Commun.* **2009**, *149*, 375.
- (32) Moc, J. *Eur. Phys. J. D* **2007**, *45*, 247.
- (33) Yao, C. H.; Zhao, S. F.; Li, J. R.; Mu, Y. W.; Wan, J. G.; Han, M.; Wang, G. H. *Eur. Phys. J. D* **2010**, *57*, 197.
- (34) Upton, T. H. *Phys. Rev. Lett.* **1986**, *56*, 2168.
- (35) Upton, T. H.; Cox, D. M.; Kaldor, A. In *The Physics and Chemistry of Small Clusters*; Jena, P., Ed.; Plenum: New York, 1987.
- (36) Jarrold, M. F.; Bower, J. E. *J. Am. Chem. Soc.* **1988**, *110*, 70.
- (37) Cui, L.-F.; Li, X.; Wang, L.-S. *J. Chem. Phys.* **2006**, *124*, 054308.
- (38) Costantino, M.; Fipro, C. *J. Mater. Res.* **1977**, *6*, 2397.
- (39) Zakorzhevskii, V. V.; Borovinskaya, I. P.; Sachkova, N. V. *Inorg.* **2002**, *38*, 1131.
- (40) Boo, B. H.; Liu, Z. *J. Phys. Chem. A* **1999**, *103*, 1250.
- (41) Andrews, L.; Zhou, M.; Chertihin, G. V.; Bare, W. D.; Hannachi, Y. *J. Phys. Chem. A* **2000**, *104*, 1656.
- (42) Kandalam, A. K.; Pandey, R.; Blanco, M. A.; Costales, A.; Recio, J. M.; Newsam, J. M. *J. Phys. Chem. B* **2000**, *104*, 4361.
- (43) Kandalam, A. K.; Blanco, M. A.; Pandey, R. *J. Phys. Chem. B* **2001**, *105*, 6080.
- (44) Averkiev, B. B.; Boldyrev, A. I.; Li, X.; Wang, L.-S. *J. Phys. Chem. A* **2007**, *111*, 34.
- (45) Averkiev, B. B.; Call, S.; Boldyrev, A. I.; Wang, L.-M.; Huang, W.; Wang, L.-S. *J. Phys. Chem. A* **2008**, *112*, 1873.
- (46) Bai, Q.; Song, B.; Hou, J.; He, P. *Phys. Lett. A* **2008**, *372*, 4545.
- (47) Romanowski, Z.; Krukowski, S.; Grzegory, I.; Porowski, S. *J. Chem. Phys.* **2001**, *114*, 6353.
- (48) Cao, B.; Starace, A. K.; Judd, O. H.; Jarrold, M. F. *J. Am. Chem. Soc.* **2009**, *131*, 2446.
- (49) Cao, B.; Starace, A. K.; Judd, O. H.; Bhattacharyya, I.; Jarrold, M. F.; Lopez, J. M.; Aguado, A. *J. Am. Chem. Soc.* **2010**, *132* (37), 12906.
- (50) Kresse, G.; Hafner, J. *J. Phys. Rev. B* **1993**, *48*, 13115.
- (51) Kresse, G.; Furthmüller, J. *Comput. Mater. Sci.* **1996**, *6*, 15.
- (52) Kohn, W.; Sham, L. J. *Phys. Rev.* **1965**, *140*, 1133.
- (53) Vanderbilt, D. *Phys. Rev. B* **1990**, *41*, 7892.
- (54) (a) Perdew, J. P.; Wang, Y. *Phys. Rev. B* **1992**, *45*, 13244. (b) Schultz, N. E.; Staszewska, G.; Staszewski, P.; Truhlar, D. G. *J. Phys. Chem. B* **2004**, *108*, 4850. (c) Budi, A.; Henry, D. J.; Gale, J. D.; Yarovsky, I. *J. Phys.: Condens. Matter* **2009**, *21*, 144206.
- (55) Payne, M. C.; Teter, M. P.; Allan, D. C.; Arias, T. A.; Joannopoulos, J. D. *Rev. Mod. Phys.* **1992**, *64*, 1045.
- (56) Pulay, P. *Chem. Phys. Lett.* **1980**, *73*, 393.
- (57) Silvi, B.; Savin, A. *Nature (London)* **1994**, *371*, 683.
- (58) Bogicevic, A.; Hyldgaard, P.; Wahnstrom, G.; Lundqvist, B. I. *Phys. Rev. Lett.* **1998**, *81*, 172.
- (59) Akola, J.; Hakkinen, H.; Manninen, M. *Phys. Rev. B* **1998**, *58*, 3601.
- (60) Boldyrev, A. I.; Schleyer, P. v. R. *J. Am. Chem. Soc.* **1991**, *113*, 9045.
- (61) Jones, R. O. *J. Chem. Phys.* **1993**, *99*, 1194.
- (62) Ojwang, J. G. O.; van Santen, R. A.; Kramer, G. J.; Van Duin, A. C. T.; Goddard, W. A., III. *J. Chem. Phys.* **2008**, *129*, 244506.
- (63) Zhang, W.; Lu, W.-C.; Sun, J.; Wang, C. Z.; Ho, K. M. *Chem. Phys. Lett.* **2008**, *455*, 232.
- (64) Drebov, N.; Alrichs, R. *J. Chem. Phys.* **2010**, *132*, 164703.
- (65) Chandrachud, P.; Joshi, K.; Kanhere, D. G. *Phys. Rev. B* **2007**, *76*, 235423.
- (66) Dahl, S.; Logadottir, A.; Egeberg, R. C.; Larsen, J. H.; Chorkendorff, I.; Törnqvist, E.; Nørskov, J. K. *Phys. Rev. Lett.* **1999**, *83*, 1814.
- (67) Rosowski, F.; Hinrichsen, O.; Muhler, M.; Ertl, G. *Catal. Lett.* **1996**, *36*, 229.
- (68) Hinrichsen, O.; Rosowski, F.; Hornung, A.; Muhler, M.; Ertl, G. *J. Catal.* **1997**, *165*, 33.
- (69) Tománek, D.; Bennemann, K. H. *Phys. Rev. B* **1985**, *31*, 2488.
- (70) Henry, D. J.; Szare, P.; Hirai, K.; Ichikawa, K.; Tachibana, A.; Yarovsky, I. *J. Phys. Chem. C* **2011**, *115*, 1714.